

ON THE OPTIMAL LOCATION OF BLEED PORTS FOR GAS TURBINE COOLING

André C. Marta*, Sriram Shankaran**

*LAETA, CCTAE, Instituto Superior Técnico, Universidade de Lisboa, Lisboa, Portugal

**Fluid Mechanics Lab, Global Research Center, General Electric, Niskayuna, NY, USA

andre.marta@tecnico.ulisboa.pt; shankaran@ge.com

Keywords: *adjoint method, sensitivity analysis, source terms, heat transfer*

Abstract

A novel approach to determine the optimal location of bleed ports for gas turbine cooling is presented. It is based on the adjoint method, thus being computationally very efficient and producing an extensive sensitivity analysis to the control variables. This approach easily evaluates every point of all surfaces (hub, blade and casing), giving the designer a new level of information for determining the optimal location that delivers the most impact in cooling at the least expense of required bleed flow.

1 Introduction

Over the last years, the most significant progress in turbomachinery have been linked to material sciences and cooling technology [1], in particular in the first rows of the high pressure turbine where the flow often exceeds the metal melting temperatures.

Advances in material science and technology have produced hundreds of different types of coatings to protect structural engineering materials from corrosion, wear, and to provide thermal insulation. Among all types, the thermal barrier coatings (TBC) are the ones used in aerospace applications, in particular to insulate turbine and combustor in gas turbine engine components from the extremely hot gas. The TBCs are typically composite material, made of metal and ceramic layers. These coatings allow the engines to operate at temperatures higher than the bare metal limit temperature, thus improving the durability and energy efficiency [2].

While the aerothermal problem has been tackled by talented designers [3], where the expertise and in-depth physical understanding leads to clever designs, the use of custom-developed numerical tools can provide to those designers a new level of knowledge that can potentially lead to more efficient gas turbines [4-8].

When it comes to optimal design, there has been several studies of the effect of vane/blade position [9] and cooling flow rates in the aerothermal performance of turbomachinery [10, 11]. While the first study was experimental using a wind tunnel, the last two were computational, but they all had in common the fact of being parametric studies, that is to say, a very restricted set of possible values were tested for the design variable at study.

To properly search the design space, and given that holistic searches are not efficient, the use of adequate numerical optimization techniques must be put in place. In such case, design of any turbomachinery component can be mathematically formulated as an optimization problem, that can be cast in non-linear programming form as

$$\begin{aligned} & \text{minimize} && f(\alpha, \omega(\alpha)) && (1) \\ & \text{w.r.t.} && \alpha \\ & \text{subject to} && \mathcal{R}(\alpha, \omega(\alpha)) = 0 \\ & && c(\alpha, \omega(\alpha)) = 0, \end{aligned}$$

where f stands for the objective (or cost) function, α is the vector of design variables and w is the state solution, which is typically of

function of the design variables, and $c = 0$ represents additional constraints that may or may not involve the state solution.

For the particular case of a CFD design problem, w is the flow solution, and the additional constraint $\mathcal{R} = 0$ represents the flow governing equations, which means that the solution must always obey the flow physics.

Among the plethora of different optimization algorithms [12], the gradient-based optimizer offer the best performance, at the expense of requiring the estimation of derivatives of the functions of interest, either objective f or constraints c of the optimization problem Eq.(1), with respect to the design variables α .

The ideal behind the goal of the present paper is to use information of the derivative of some aerothermal turbomachinery performance metrics with respect to the location of the cooling bleed ports, to assess the optimal location of flow injection or extraction, to improve those desired metrics. The approach proposed is based on a novel extension of the adjoint method, that is already routinely employed in many aerodynamic shape optimization problems, both of external aircraft flows [13] and internal turbomachinery flows [14,15].

The paper is organized in four main sections. First, the aerothermal analysis solver is briefly described and the relevant performance metrics are introduced. Then, the adjoint formulation is presented, with particular focus to the new extension to the modeling of bleed flow and the derivation of the sensitivity analysis equations for such case. Next, a representative test case is used to demonstrate the suggested method and prove its efficiency and accuracy. Lastly, some overall conclusions are drawn from the results obtained, together with the suggestion of a possible aerothermal design framework incorporating the method proposed to solve the optimization problem in the form of Eq.(1) using a gradient-based optimization algorithm.

2 Aero-Thermal Analysis

2.1 Flow Solver

The governing equations used in the present work are the Reynolds-Averaged Navier-Stokes (RANS) equations. In conservation form, the system of equations may be written in index notation as:

$$\frac{\partial \rho}{\partial t} + \frac{\partial}{\partial x_j} (\rho u_j) = 0 \quad (2)$$

$$\frac{\partial}{\partial t} (\rho u_i) + \frac{\partial}{\partial x_j} (\rho u_i u_j + p \delta_{ij} - \tau_{ji}) = 0 \quad (3)$$

$$\frac{\partial}{\partial t} (\rho E) + \frac{\partial}{\partial x_j} (\rho E u_j + p u_j - u_i \tau_{ij} + q_j) = 0 \quad (4)$$

where ρ , u_i and E are respectively the density, mean velocity and total energy, p is the pressure, τ_{ij} is the viscous stress and q_j is the heat flux.

The k - ω turbulence model [16] is used to model the Reynolds stresses:

$$\begin{aligned} \frac{\partial}{\partial t} (\rho k) + \frac{\partial}{\partial x_j} (\rho k u_j) &= \tau_{ij} \frac{\partial u_i}{\partial x_j} - \beta_k \rho k \omega + \quad (5) \\ &\frac{\partial}{\partial x_j} \left[\left(\mu + \sigma_k \frac{\rho k}{\omega} \right) \frac{\partial k}{\partial x_j} \right] \end{aligned}$$

$$\begin{aligned} \frac{\partial}{\partial t} (\rho \omega) + \frac{\partial}{\partial x_j} (\rho \omega u_j) &= \frac{\gamma \omega}{k} \tau_{ij} \frac{\partial u_i}{\partial x_j} - \beta_\omega \rho \omega^2 + \quad (6) \\ &\frac{\partial}{\partial x_j} \left[\left(\mu + \sigma_\omega \frac{\rho k}{\omega} \right) \frac{\partial \omega}{\partial x_j} \right] \end{aligned}$$

where k is the turbulence kinetic energy and ω is the specific dissipation rate. The turbulent eddy viscosity is computed from $\mu_T = \rho k / \omega$ and the constants are $\gamma = 5/9$, $\beta_k = 9/100$, $\beta_\omega = 3/40$, $\sigma_k = 1/2$ and $\sigma_\omega = 1/2$. The effective viscosity used in the Navier-Stokes (Eqs. 2-4) is then computed as $\mu = \mu_m + \mu_T$, where μ_m is the molecular (laminar) viscosity.

In semi-discrete form, the RANS governing equations (Eqs.1-5) can be expressed as

$$\frac{dw_{ijk}}{dt} + \mathcal{R}_{ijk}(w) = 0 \quad (7)$$

where $w = (\rho, \rho u, \rho E, \rho k, \rho \omega)^T$ is the vector of conservative variables, \mathcal{R} is the residual with all of its components (inviscid, viscous and turbulent fluxes, boundary conditions and artificial dissipation). The unsteady term in Eq. (7) is dropped out since only the steady solution is of interest in this work.

A finite volume formulation is used to numerically discretize Eq.(7) in structured grids, in a proprietary three-dimensional, multi-block flow solver. Details of the numerical techniques employed can be found in reference [17].

2.2 Bleed Flow Modeling

The bleed flow is modeled with additional source terms \mathcal{S} included in the continuity, momentum and energy equation:

$$\tilde{\mathcal{R}} = \mathcal{R} + \mathcal{S} \quad (8)$$

The terms can either be fully specified (all seven terms corresponding to mass, momentum, energy and turbulence) or only mass (being the remaining six terms computed using the local flow conditions). The sign of the additional vector is used to distinguish between source and sink terms, corresponding to flow injection and extraction, respectively.

It should be noted that the approach detailed is general, making it applicable to any sort of modeling of the cooling flow, here represented by the vector \mathcal{S} of source terms.

2.3 Performance metrics

Among the several metrics that can be used to quantify the performance of a turbomachinery blade, focus will be given to some representative aerodynamic quantities, like rotor pressure ratio and efficiency or stator loss coefficient, and some thermal quantities, like averaged or maximum temperature on specified surface patch.

In this work, two metrics \mathcal{F} were selected: the isentropic efficiency, defined as

$$\eta = \frac{(p_{Ta}^{exit}/p_{Ta}^{inlet})^{(\gamma-1)/\gamma} - 1}{(T_{Ta}^{exit}/T_{Ta}^{inlet}) - 1} \quad (9)$$

where the pressure p is enthalpy-averaged and the temperature T is mass-averaged at the inlet or exit sections, and the subscript Ta refers to a total absolute quantity; and the area-averaged gas total temperature using a user-selected surface region Ω , estimated as

$$T_{Ta}^{\Omega} = \frac{\int \left(T_S + \frac{1}{2C_P} (u_i u_i) \right) d\Omega}{\int d\Omega} \quad (10)$$

where the static temperature is evaluated from the vector of conservative variables w using an equation of state of the working gas. For simplicity, an ideal gas is assumed, thus $T_S = p/(\rho R)$, where R is the gas constant, being the pressure and density quantities evaluated at the surface. Furthermore, in the test case shown ahead, the selected surface region corresponds to the whole blade, including both suction and pressure sides.

3 Optimal Location of Bleed Ports

3.1 Adjoint Method

The adjoint equations can be derived using the approach by Giles [18] leading to

$$\left[\frac{\partial \tilde{\mathcal{R}}}{\partial w} \right]^T \psi = \frac{\partial \mathcal{F}}{\partial w} \quad (11)$$

The performance metrics vector $\mathcal{F} = \mathcal{F}(w, \mathcal{S})$ is a function of the state variables w and the source terms \mathcal{S} , that in our approach take the role of control (design) variables.

The implementation of the adjoint solver follows the procedure found in [19], where the flow solver code that evaluates the residual \mathcal{R} and metric functions \mathcal{F} are automatically differentiated with respect to the state variables w to obtain the routines to evaluate the entries of the matrix and right-hand side vector in Eq.(11).

It should be noted that Eq.(11) is the usual adjoint equation, thus the adjoint solution ϕ can be used from an existing adjoint solver

developed with any other purpose in mind, such as shape optimization. The difference of the purposed approach lies in the step describe subsequently.

3.2 Sensitivity Analysis

The adjoint-based sensitivity of the performance metrics to the bleed flow is given by

$$G = \frac{d\mathcal{F}}{d\mathcal{S}} = \frac{\partial\mathcal{F}}{\partial\mathcal{S}} - \psi^T \left[\frac{\partial\tilde{\mathcal{R}}}{\partial\mathcal{S}} \right] \quad (12)$$

In contrast to the adjoint system in Eq.(11), the influence of the design variables shown in the gradient expression in Eq.(12), through the vector and matrix of partial derivatives.

Similarly to the assembly of the terms in Eq.(11), the computational routines to evaluate $d\mathcal{F}/d\mathcal{S}$ and $d\tilde{\mathcal{R}}/d\mathcal{S}$ were also obtained by means of automatic differentiation, again following the methodology described in reference [19].

This adjoint-based process allows for elimination of the terms that depend on the flow solution with the result that the gradient with respect to an arbitrary number of design variables can be determined without the need for additional evaluations of the flow state.

3.3 Criteria for Optimal Location Detection

Solving Eq.(8) for the adjoint field ψ , the sensitivity of \mathcal{F} can be estimated at every surface location on the domain (hub, blade or casing) from Eq.(9). By identifying the regions where the sensitivity is the highest (positive) and lowest (negative), those correspond to the location of the injection and extraction bleed ports, respectively, to optimally increase the performance metric of interest with the minimum bleed flow required.

If different metrics point to different directions, it is up to the designer to evaluate possible trade-offs or to use a numerical optimization tool, to solve the problem in either multi-objective or constrained single-objective form, as detailed in Sec.5.

4 Results and Discussion

The approach documented in the previous sections is demonstrated in a test case consisting in the blade passage of a high-pressure turbine (HPT) rotor.

The front and side views of the turbine rotor disk of the modeled gas turbine engine are shown in Fig.1.

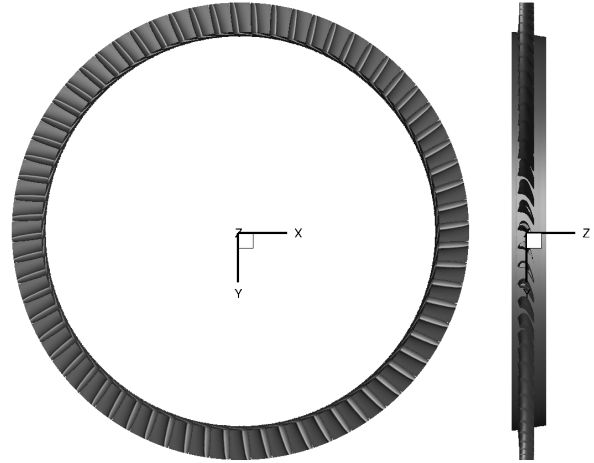


Fig. 1. Turbine rotor disk (left: front view, right: side view).

Since only the steady solution is of interest for the present analysis, a single blade passage of the HPT rotor is modeled, as illustrated in Fig.2.

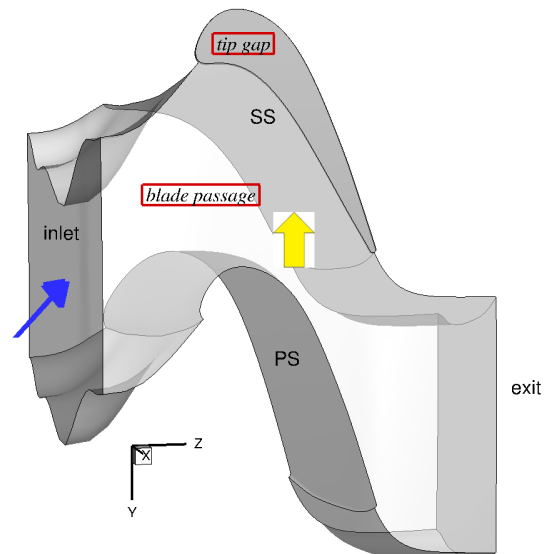


Fig. 2. Computational domain.

The flow goes from left to right (blue arrow) and the blade is rotating with negative angular velocity in the z-axis.

The blade section side (SS) and pressure side (PS), as well as the hub (x_{min}) and casing surfaces (x_{max}), are modeled as no-slip wall boundaries. Total pressure and temperature are prescribed at the inlet, and static pressure is extrapolated at the exit. Besides the blade passage domain, an additional computational domain is used to physically model the tip gap. The remaining boundaries are periodic.

The main flow is shown in Fig.3 and Fig.4. for pressure and absolute velocity field, respectively, on a plane cut at 50% blade span.

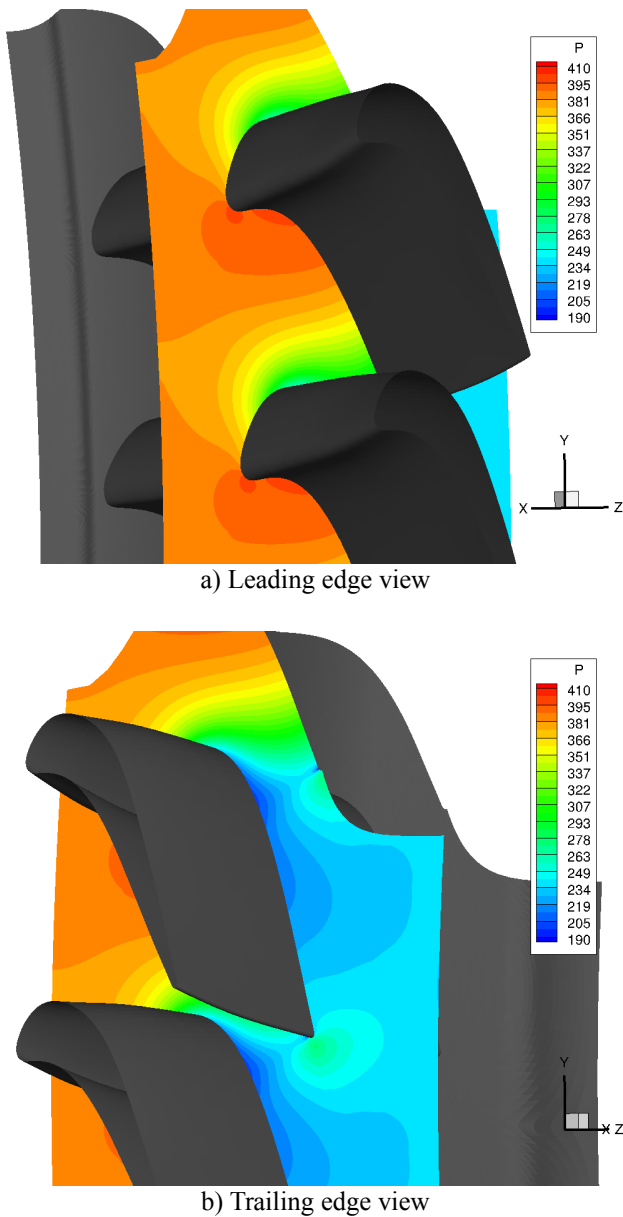


Fig. 3. Pressure contour in 50% blade span plane.

The hub surface is in the foreground and the blade passage solution was replicated for visualization purposes.

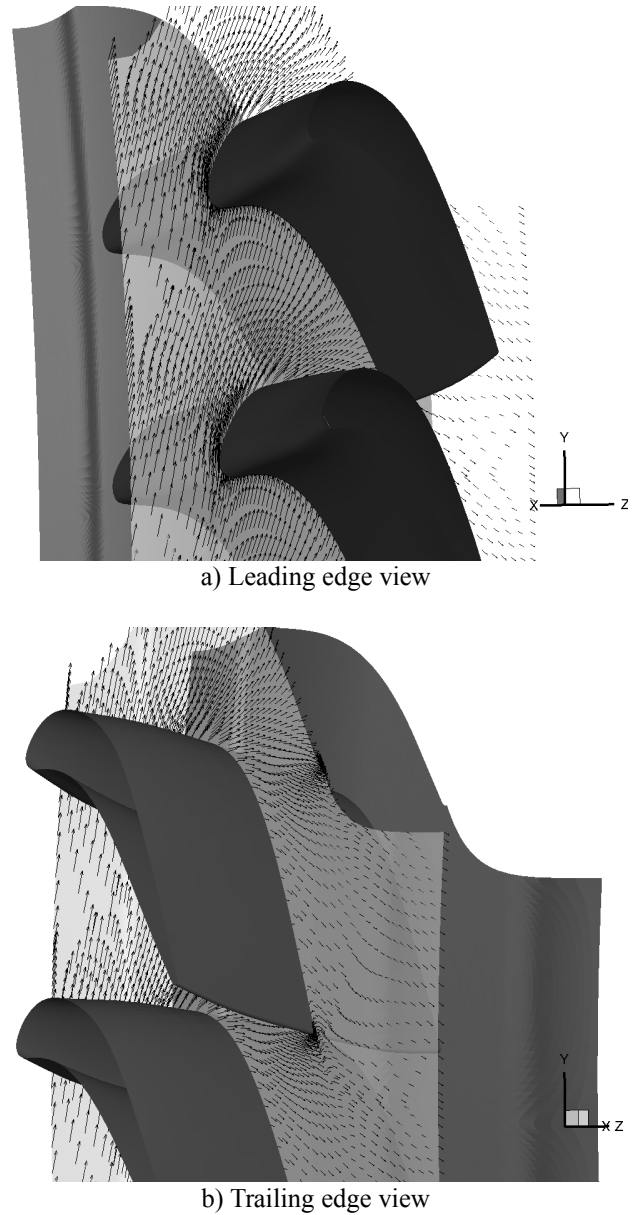


Fig. 4. Velocity field in 50% blade span plane.

The density distribution and the momentum vector for the modeled HPT blade passage are shown in figures 5 and 6, respectively for the main and bleed flows.

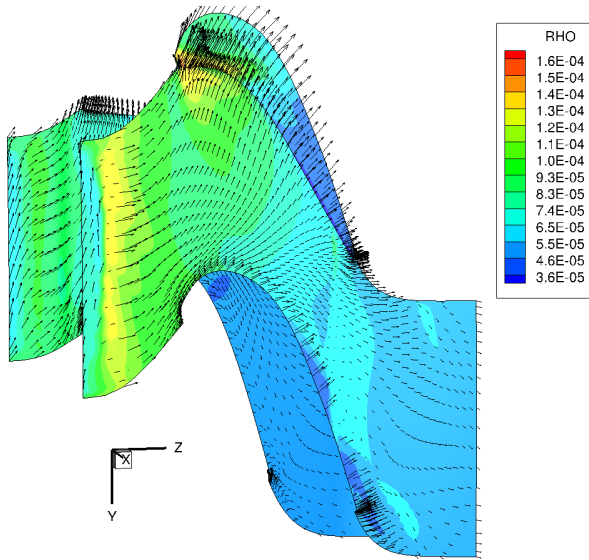


Fig. 5. Density flow field.

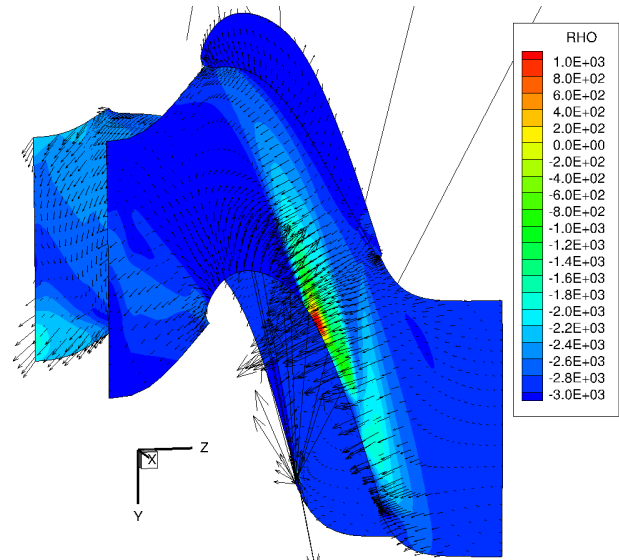


Fig. 7. Rotor hub, casing and blade tip surfaces: adjoint solution for the isentropic efficiency.

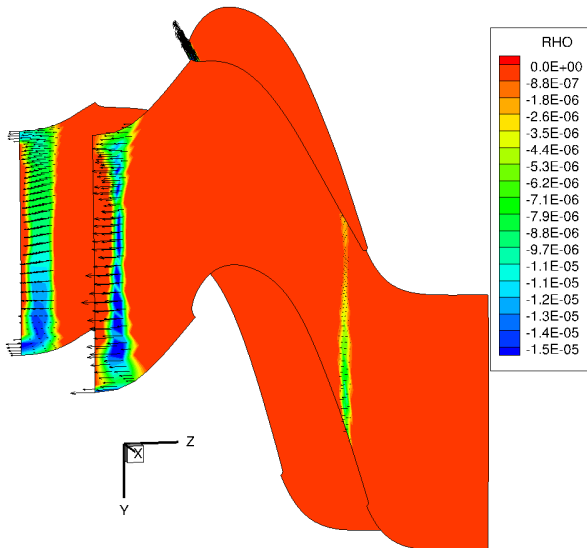


Fig. 6. Rotor blade passage: mass source terms.

It should be noticed that, according to the implementation of the CFD solver, the source terms \mathcal{S} are subtracted (negative sign in Eq.(8)), thus the negative values in Fig.6 represent flow injection. As such, flow is being injected simultaneously in four regions: holes at the hub and casing located upstream of the blade LE; at the blade tip LE; and also at the casing immediately after the blade TE.

The solution of Eq.(11) is graphically shown in figures 7 and 8. Despite being a volume solution, the adjoint vector ψ is only shown at some selected surfaces, namely hub, casing and blade tip, since these are the regions of interest for the cooling bleed flow analysis.

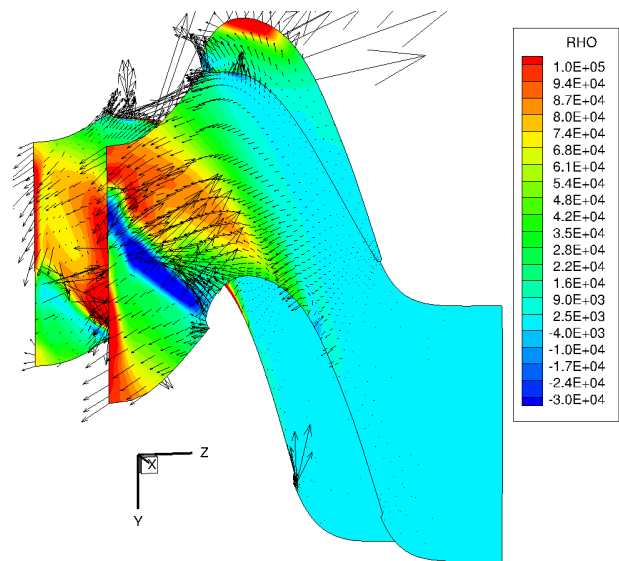


Fig. 8. Rotor hub, casing and blade tip surfaces: adjoint solution for the blade average absolute total temperature.

From the adjoint solution for the blade average absolute total temperature shown in Fig.8, it becomes clear that the impact on the blade temperature comes only from the region located upstream, as one would easily acknowledge from basic principles of fluid mechanics and thermodynamics.

In this test case, the source terms were simplistically modeled as an imposed state vector at the mentioned wall surfaces. Consequently, the adjoint-based gradient Eq. (12) reverts to the actual adjoint solution: the term $d\mathcal{F}/d\mathcal{S}$ is zero because there is no explicit dependency of the functions of interest on the source terms; and the term $d\mathcal{R}/d\mathcal{S}$ simplifies to the negative of the identity matrix by means of Eq.(8), since the bleed flow injection is represented by a negative quantity.

temperature Eq. (10), with respect to the bleed mass (RHO) are shown in figures 9 and 10. respectively, at the hub and casing surfaces. In those surfaces, regions of positive sensitivity indicate that increasing \mathcal{S} would result in increased \mathcal{F} . Since the source term implementation uses negative \mathcal{S} for modeling the cooling injection, then it means that: for regions of positive sensitivity, placing extraction (sinks) holes or slots would result in an increase of the assessed metric; for regions of negative sensitivity, placing injection (sources) holes or slots would result in an increase of the assessed metric.

The overall negative sensitivity of the isentropic efficiency with respect to the bleed mass shown in Fig.9 reveal that adding or increasing flow injection (making \mathcal{S} even more negative) would result in an increased rotor blade passage efficiency. This conclusion is not as straightforward as that, since the effect of the added bleed flow would have to be accounted in the computation of the corrected blade passage efficiency. It is interesting to notice a region on the blade PS where flow extraction would be beneficial in terms of efficiency.

As for the sensitivity of the blade average absolute total temperature with respect to the bleed mass shown in Fig.10, one fact stands out: the effect of injecting or extracting flow from the hub or casing surfaces fades out as the location moves downstream, as one would immediately acknowledge since the transport caused by the main flow would prevent the bleed flow from impacting the blade. Focusing on the hub surface (Fig.10(a)), a significant reduction of the blade temperature can be achieved by placing injection ports/slots in the vicinity of the blade LE, in the regions identified with green to red contour levels (corresponding to positive sensitivity), being more effective if located closer to the fore portion of the blade SS. The potential of using the casing to place bleed ports/slots for blade temperature reduction can be inferred from Fig.10(b). Again, the regions identified with green to red contour levels correspond to reduction of blade temperature by the addition or increase of flow injection. Compared to the hub surface, there is an important difference in

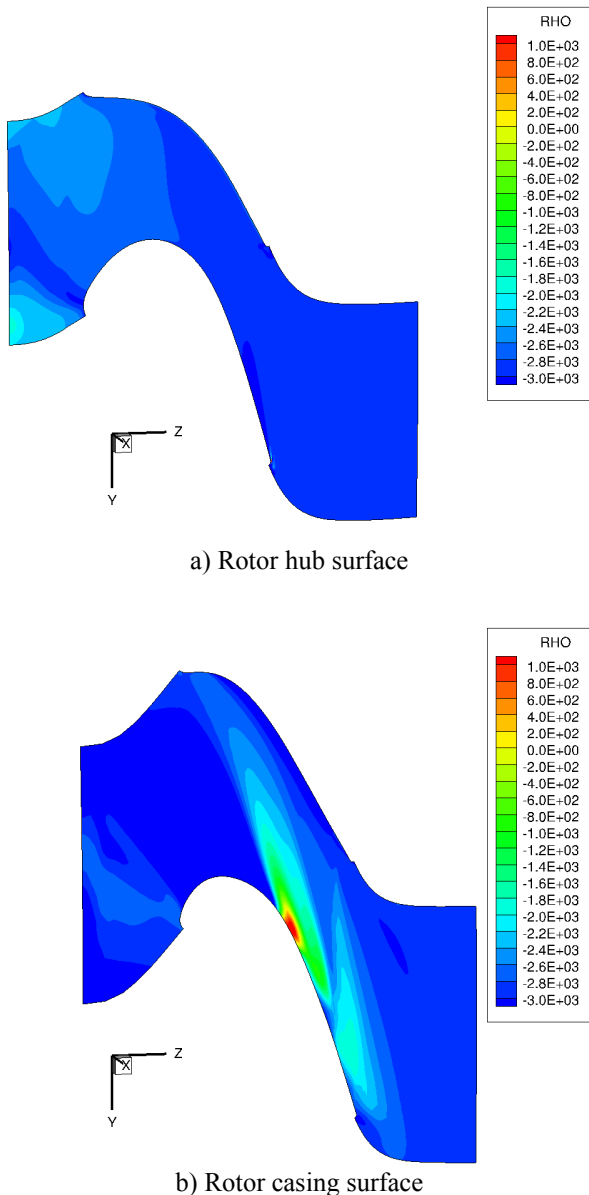


Fig. 9. Isentropic efficiency sensitivity to bleed mass.

The sensitivity of the selected performance metrics, isentropic efficiency Eq. (9) and the blade average absolute total

that there is a region (dark blue contour) where injection has a negative impact. In that region, flow extraction leads to the desired reduction in blade temperature.

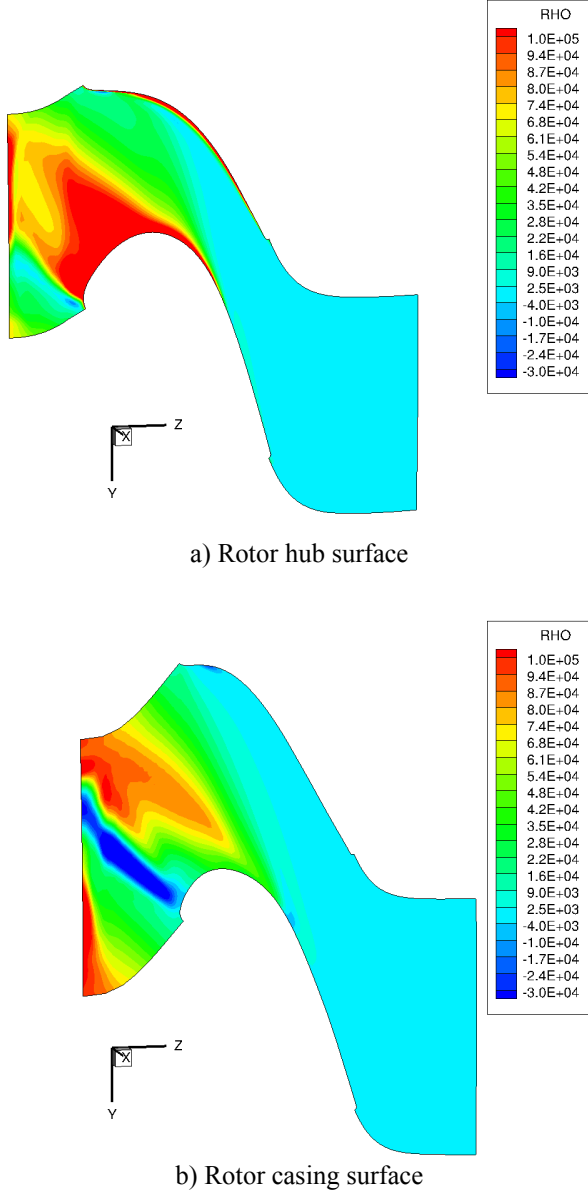


Fig. 10. Blade average absolute total temperature sensitivity to bleed mass.

Comparing the sensitivity of both performance metrics, and assuming that the goal is to increase efficiency (regions of dark blue contours in Fig.9) and decrease blade temperature (regions of red contours in Fig.10), the present test case exhibits solutions that can achieve just that if one chooses to place injection holes/slots in the hub surface in vicinity of the blade LE closer to the fore

portion of the blade SS, and in the casing surface at the blade LE streamwise location. Regions of conflicting performance metric sensitivities would require a more careful analysis, involving trade-off considerations.

5 Aerothermal Design Framework

The discussion of the best location of injection or extraction holes/slots in Sec.4 was based on direct observation of the adjoint-based sensitivities. The inclusion of this detailed sensitivity analysis capability in an optimization tool can be desired for dealing with more complex problems or to automatize the solution process.

In that in mind, a conceptual aerothermal design framework is presented in Fig.11.

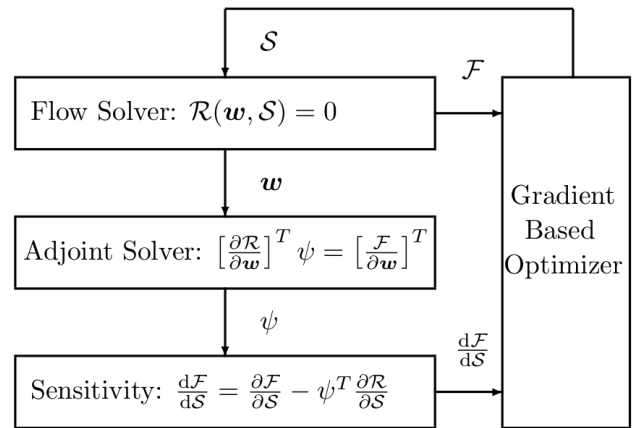


Fig. 11. Gradient-based aerothermal design framework.

The analysis capability of the framework is composed of three blocks: flow solver and sensitivity analysis. Given a particular source term model \mathcal{S} , the flow solution w can be computed by solving the governing equations Eq.(7) and then the values of the functions of interest \mathcal{F} can be estimated. The adjoint vector ψ is then be obtained by solving the adjoint Eq.(11). Finally, using this solution, the gradient of the functions of interest is evaluated using Eq.(12).

The design capability of the framework comes from the presence of an optimizer, in particular a gradient-based optimizer. The coupling of the analysis module to this optimization block, involves receiving both the value and gradient of the functions of interest from the former, and in turn providing a new

solution \mathcal{S} to drive the solution to improve the objective in Eq.(1). Upon convergence of the optimizer, the best bleed flow properties (location and intensity) can be achieved.

Lastly, not represented in the architecture shown in Fig.11, it is desired to add an additional layer module to transform the adjoint design variables \mathcal{S} into some manufacturing parameters, like streamwise, tangential and radial position coordinates, hole diameter or slot gap, and inlet/exit bleeding port orientation. This choice is tightly connected to the legacy cooling design practice.

6 Conclusions

A novel approach to assess the best location of cooling bleed flow injection was presented. The use of the adjoint method provides a detailed sensitivity analysis that can ultimately be used together with numerical optimization techniques to accurately and efficiently determine the best location of the injection or extraction holes or slots.

This approach has the potential to expedite and considerably reduce the costs associated with the aerothermal design of gas turbine engines, in particular for the ever complex first stage HPTs.

The adjoint-based formulation presented is generic and it can be applied to any type of bleed flow modeling used in the CFD analysis. If there is already a legacy adjoint solver developed for shape optimization, the additional programming effort required to implement the proposed approach is vastly reduced since Eq. (11) is already solved. In that case, only the explicit dependency of the residual of the flow governing equations and the functions of interest on the source terms need to be considered to evaluate the new terms $d\mathcal{F}/d\mathcal{S}$ and $d\mathcal{R}/d\mathcal{S}$ in the adjoint-based sensitivity expression Eq.(12).

References

- [1] Han J-C, Dutta S and Ekkad S. *Gas Turbine Heat Transfer and Cooling Technology*. 2nd edition, CRC Press, 2013. ISBN:9781439855683
- [2] Padture N P, Gell M and Jordan E H. Thermal Barrier Coatings for Gas-Turbine Engine Applications. *Science*, Vol.296, No.5566, pp.280-284, 2002. DOI:10.1126/science.1068609
- [3] Walsh P P and Fletcher P. *Gas Turbine Performance*. 2nd edition, Blackwell Science, 2004. ISBN:978-0632064342
- [4] Fransen R, Gourdain N and Gicquel, L. Steady and unsteady modeling for heat transfer predictions of high pressure turbine blade internal cooling. In ASME Turbo Expo 2012, Copenhagen, 2012, GT2012-69482. DOI:10.1115/GT2012-69482
- [5] Wang G, Duchaine F, Papadogiannis D, Duran I, Moreau S and Gicquel L. An overset grid method for large eddy simulation of turbomachinery stages. *Journal of Computational Physics*, Vol.274, pp.333-355, 2014. DOI:10.1016/j.jcp.2014.06.006
- [6] Tucker P. Trends in turbomachinery turbulence treatments. *Progress in Aerospace Sciences*, Vol.63, pp.1-32, 2013. DOI:10.1016/j.paerosci.2013.06.001
- [7] De Maesschalck C, Lavagnoli S, Paniagua G and Vinha N. Aerothermodynamics of tight rotor tip clearance flows in high-speed unshrouded turbines. *Applied Thermal Engineering*, Vol.65, No.1-2, pp.343-351, 2014. DOI:10.1016/j.applthermaleng.2014.01.015
- [8] Morata E, Gourdain N, Duchaine F and Gicquel L. Effects of free-stream turbulence on high pressure turbine blade heat transfer predicted by structured and unstructured LES. *International Journal of Heat and Mass Transfer*, Vol.55, No.21-22, pp.5754-5768, 2012. DOI:10.1016/j.ijheatmasstransfer.2012.05.072
- [9] Rhee D-H and Cho H. Effect of vane/blade relative position on heat transfer characteristics in a stationary turbine blade: Part 2. Blade surface. *International Journal of Thermal Sciences*, Vol.47, No.11, pp.1544-1554, 2008. DOI:10.1016/j.ijthermalsci.2007.12.007
- [10]Huo W and Yan X. Effects of coolant flow rates on cooling performance of the intermediate pressure stages for an ultra-supercritical steam turbine. *Applied Thermal Engineering*, Vol.62, No.2, pp.723-731, 2014. DOI:10.1016/j.applthermaleng.2013.09.012.
- [11]Gao J, Zheng Q, Zhang Z and Jiang Y. Aero-thermal performance improvements of unshrouded turbines through management of tip leakage and injection flows. *Energy*, Vol.69, pp.648-660, 2014. DOI:10.1016/j.energy.2014.03.060
- [12]NocedalJ and Wright S. *Numerical Optimization*. 2nd edition, Springer, 2006. ISBN:9780387303031

- [13]Martins J R R A, Alonso J J and Reuther J J. High-fidelity aerostructural design optimization of a supersonic business jet. *Journal of Aircraft*, 41(3):523–530, 2004. DOI:10.2514/1.11478.
- [14]Luo J, Zhou C and Liu F. Multipoint design optimization of a transonic compressor blade by using an adjoint method. *Journal of Turbomachinery*, 136(5):051005, 2014. DOI:10.1115/1.4025164.
- [15]Marta A C ,Shankaran S, Venugopal P, Barr B and Wang Q, Interpretation of Adjoint Solutions for Turbomachinery Flows, *AIAA Journal*, Vol.51, No.7, pp.1733-1744, 2013. DOI: 10.2514/1.J052177
- [16]Wilcox D C. *Turbulence Modeling for CFD*, 2nd edition, DCW Industries Inc, 2002. ISBN: 978-1928729105
- [17]Holmes D G, Mitchell B E and Lorence C B. Three dimensional linearized Navier-Stokes calculations for flutter and forced response. In T H Fransson (ed.), *Unsteady Aerodynamics and Aeroelasticity of Turbomachines*, Vol.4, pp.211-224. Springer, 1998. DOI:10.1007/978-94-011-5040-8_14
- [18]Giles M B and Pierce N A. An introduction to the adjoint approach to design. *Flow, Turbulence and Combustion*, Vol.65, pp.393-415, 2000. DOI:10.1023/A:1011430410075
- [19]Marta A C, Van der Weide E, Alonso J J, Mader C A and Martins J R R A, ADjoint: A methodology for the development of discrete adjoint solvers using automatic differentiation tools, *International Journal of Computational Fluid Dynamics*, Vol.21, No.9-10, pp.307-327, 2007. DOI:10.1080/10618560701678647
- [20]Marta A C and Shankaran S, On the Handling of Turbulence Equations in RANS Adjoint Solvers, *Computers & Fluids*, Vol.74, pp.102-113, 2013. DOI: 10.1016/j.compfluid.2013.01.012

Copyright Statement

The authors confirm that they, and/or their company or organization, hold copyright on all of the original material included in this paper. The authors also confirm that they have obtained permission, from the copyright holder of any third party material included in this paper, to publish it as part of their paper. The authors confirm that they give permission, or have obtained permission from the copyright holder of this paper, for the publication and distribution of this paper as part of the ICAS 2014 proceedings or as individual off-prints from the proceedings.